Article

Biocompatible and antibacterial nitric oxide-releasing Pluronic F-127/chitosan hydrogel for topical applications

Milena T. Pelegrino [1,2], Bruna de Araujo Lima [3], Mônica H. M. do Nascimento [1,2], Christiane B. Lombello [1,2], Marcelo Brocchi[3], Amedea B. Seabra [1,2,*]

[1]   Center for Natural and Human Sciences, Universidade Federal do ABC, Av. dos Estados 5001, CEP 09210-580, Santo André, SP, Brazil

[2]   Nanomedicine Research Unit (NANOMED), Universidade Federal do ABC, Santo André, SP, Universidade Federal do ABC, Av. dos Estados 5001, CEP 09210-580, Santo André, SP, Brazil

[3]   Tropical Disease Laboratory, Department of Genetics, Evolution, Microbiology and Immunology, Institute of Biology, University of Campinas, SP, Brazil

*   Correspondence: amedea.seabra@ufabc.edu.br; Tel.: +55-11-4996-8374

Abstract: Nitric oxide (NO) is involved in physiological processes, including vasodilatation, wound healing and antibacterial activities. As NO is a free radical, designing drugs to generate therapeutic amounts of NO in controlled spatial and time manners is still a challenge. In this study, the NO donor S-nitrosoglutathione (GSNO) was incorporated into the thermoresponsive Pluronic F-127 (PL) - chitosan (CS) hydrogel, with an easy and economically feasible methodology. CS is a polysaccharide with known antimicrobial properties. Scanning electron microscopy, rheology and differential scanning calorimetry techniques were used for hydrogel characterization. The results demonstrated that the hydrogel has a smooth surface, thermoresponsive behavior and good mechanical stability. The kinetics of NO release and GSNO diffusion from GSNO-containing PL/CS hydrogel demonstrated a sustained NO/GSNO release, in concentrations suitable for biomedical applications. The GSNO-PL/CS hydrogel demonstrated a concentration-dependent toxicity to Vero cells, and antimicrobial activity to *Pseudomonas aeruginosa* (minimum inhibitory concentration and minimum bactericidal concentration values of 0.5 $\mu g \cdot mL^{-1}$ of hydrogel, which corresponds to 1 $mmol \cdot L^{-1}$ of GSNO). Interestingly, the concentration range in which the NO-releasing hydrogel demonstrated an antibacterial effect was not found to be toxic to the Vero mammalian cell. Thus, the GSNO-PL/CS hydrogel is a suitable biomaterial for topical NO delivery applications.

Keywords: Chitosan; Thermoresponsive hydrogel; Nitric oxide; S-nitrosothiols; Biocompatibility; Antimicrobial; *Pseudomonas aeruginosa*; Pluronic F127.

1. Introduction

Nitric oxide (NO) is an endogenous molecule involved in several biological signaling pathways. At low concentrations (pico- to nanomolar), NO has regulatory functions, such as the promotion of vasodilation, wound healing, cell proliferation, inhibition of platelet adhesion and aggregation [1-3]. At higher concentrations (micro- to millimolar), NO has antitumor and antimicrobial effects [2-4]. NO is considered a promising alternative to conventional antimicrobials. However, it is a challenge to deliver a precise NO concentration directly to the target site of application, in sustained and convenient manners and with minimal side effects [1].

NO is a free radical (half-life 1-5 s), and can be inactivated in biological systems upon reaction with biomolecules (such as hemoglobin), thus limiting its effects. To overcome this issue, several NO-releasing biomaterials have been prepared to carry and deliver therapeutic amounts of NO for different biomedical applications [4]. In topical applications, NO-releasing biomaterials can

be used for coating medical devices [5]. In dermatological applications, it can be used to promote dermal blood flow [6-9], for antimicrobial effects [2, 10, 11], cell proliferation [4], wound repair [12-15], controlling inflammatory pain [16] and local warming [17]. In addition, administration of NO-releasing materials on human skin might have a therapeutic effect against endothelial dysfunctions, such as vasoconstriction, vasospasm and thrombosis [5, 16, 18].

In this context, there is great interest in the development of NO-releasing biomaterials capable of releasing NO/NO donors in a controllable manner for topical applications. In this study, the NO donor S-nitrosoglutathione (GSNO) was incorporated into a thermoresponsive hydrogel comprised of poly(ethylene oxide)- poly(propylene oxide)- poly(ethylene oxide), PEO-PPO-PEO (Pluronic F127) and chitosan (CS) (Figure 1).
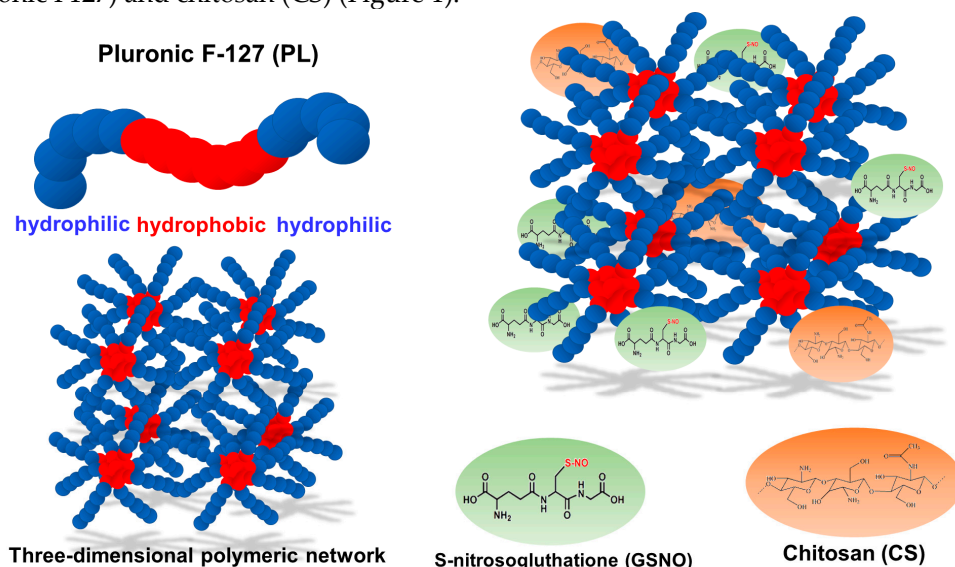

Figure 1. Schematic representation of the formation of three-dimensional polymeric network of Pluronic F-127 (PL) hydrogel structure containing chitosan (CS) and S-nitrosoglutathione (GSNO) to delivery NO.

GSNO is an endogenous molecule that spontaneously releases free NO [1, 2]. Hydrogels are soft materials with a three-dimensional network and viscoelastic properties. Thermoresponsive hydrogels can change their rheological properties with changes in temperature [19]. Pluronic (PL) is approved for human uses by the Food and Drug Administration (FDA), and has been extensively employed as a drug carrier and for tissue engineering [20]. Pluronic has also been found to decrease the viscosity of the blood, prevent aggregation of erythrocytes and adhesion to the vascular endothelium layer [21]. Due to the differences in water solubility between PEO and PPO units, PL can form micelles in aqueous solutions [22-24]. At low temperatures (0-5°C), PL behaves like a low-viscosity liquid, whereas at higher temperatures (room, physiological temperatures, for example) it has a gel-like behavior [22,23]. This feature is suitable for pharmacological formulations, since it is possible to incorporate active drugs at low temperature, and the increase in the temperature leads to the formation of a hydrogel containing the drug. The main advantage of PL hydrogels is the ease of preparation, that does not require the use organic solvents [21].

The polysaccharide chitosan (CS) was incorporated into PL hydrogel. CS is biodegradable, biocompatible, non-allergenic and an inexpensive biological polymer extensively used for tissue engineering and drug delivery [25-27]. Chitosan is obtained from chitin, which is the major component in crustacean shells, such as crabs and insects [26], so its use in technological products is of ecological and sustainable importance [28]. In addition, CS has important effects, such as antimicrobial, anticholesterolemic, antitumor, hemostatic and antioxidant activities [25-27].

The main aim of this study was to incorporate the NO donor GSNO into a thermoresponsive hydrogel composed of PL/CS (Figure 1) for topical applications. Our results demonstrated a sustained NO/NO donor release from the hydrogel matrix, at therapeutic levels. The combination of

82 NO and CS demonstrated a synergistic effect against *Pseudomonas aeruginosa.* Interestingly, the
83 concentration of NO-releasing hydrogel required for an antibacterial effect was not toxic towards
84 mammalian cells, indicating the promising and safe uses of this biomaterial in topical applications.

85 **2. Materials and Methods**

86 *2.1 Materials*

87   Chitosan (CS, low molecular weight, 75% deacetylation), glutathione (GSH), sodium nitrite
88 (NaNO2), Pluronic F-127 (PL) ([poly(ethylene oxide)]106[poly(propylene oxide)]70[poly(ethylene
89 oxide)]106, molar weight of 12,600 kDa), phosphate buffer saline (PBS, pH 7.4), MTT
90 (3-(4,5-dimethylthiazol-2-yl)-2,5-diphenyltetrazolium bromide) and phenol were obtained from
91 Sigma-Aldrich (St. Louis, MO, USA). Acetone, hydrochloric acid and lactic acid were obtained from
92 Labsynth (Diadema, SP, Brazil). All experiments were carried out using analytical grade water from
93 a Millipore Milli-Q Gradient filtration system (resistivity below 18.2 M ·cm-1 at 25.0°C). The Vero
94 cell line was obtained from Instituto Adolfo Lutz (São Paulo, SP, Brazil). The culture medium,
95 supplements, antibiotics and bovine fetal serum were obtained from Cultilab (Campinas, SP, Brazil).
96 The Mueller-Hinton media (broth and agar) were purchased from Difco (Franklin Lakes, USA), and
97 the sodium chloride (NaCl, P.A. grade), used to obtain saline solution 0.85% w/v, was purchased
98 from J.T. Baker (Ciudad del Mexico, Mexico).
99

100 *2.2 Preparation of PL/CS hydrogel*

101   PL/CS hydrogel was prepared based on the cold method first described by Schmolka et al.
102 [29]. This method has been reported extensively for the preparation of PL based hydrogels
103 containing drugs, particles or other polymers [27,30-32]. First, 0.1 g of CS was dissolved in 10 mL of
104 lactic acid (2%) under magnetic stirring at room temperature. Next, 2.0 g of PL was gradually added
105 to the CS solution under gentle magnetic stirring. The temperature was maintained at 4ºC until
106 complete dissolution of PL powder [20]. The final concentrations of PL and CS in the hydrogel were
107 20% w/v and 1% w/v, respectively. This material is referred as PL/CS hydrogel.
108

109   *2.3 Synthesis of GSNO*
110   GSNO was synthesized as previously described [33-35]. GSH (1,228 mol·L-1) was dissolved into
111 HCl (1 mol·L-1), followed by the addition of an equimolar amount of NaNO2, correlated to GSH.
112 The nitrosation reaction was carried out for 20-30 min, in an ice bath, under magnetic stirring and in
113 the dark, leading to the formation of a pink precipitate of GSNO. This material was washed with
114 cold water and filtered under vacuum using a Millipore cellulose membrane. The obtained GSNO
115 was freeze-dried for 24 h. Solid GSNO was maintained in a recipient with humidity controlled at -
116 20°C [22].
117

118   *2.4 Incorporation of GSH or GSNO into PL/CS hydrogel*
119   GSH or GSNO were incorporated into the PL/CS hydrogel matrix following the process
120 described by Pelegrino et al. with modifications [33]. The required amount of GSH or GSNO was
121 added to the PL/CS solution, under gentle magnetic stirring and light protection, at 5ºC. This
122 mixture was maintained at 5ºC until the complete dissolution of the GSH or GSNO. This process led
123 to the formation of a PL/CS hydrogel, at room temperature (final concentrations of PL and CS were
124 20% and 1% of CS w/v, respectively) containing 50 mmol·L-1 of GSH or GSNO (final concentration).
125 This is henceforth referred to as GSH-PL/CS hydrogel or GSNO-PL/CS hydrogel, respectively.
126

127   *2.5 Morphological characterization of PL/CS and GSH-PL/CS hydrogels*
128   The morphology of the PL/CS and GSH-PL/CS hydrogels was investigated by scanning
129 electron microscopy (SEM). Prior the analysis, the samples were frozen at -80°C for 12 h and
130 freezer-dried for 36 h (Labconco, 84C), as previously described [24, 36-38]. The dried materials were

131 spread on a double-sided conduction adhesive tape, pasted on a metallic stub and analyzed using a
132 benchtop SEM (JCM-6000PLUS NeoScope, JEOL Technics, Tokyo, Japan). The analysis was done
133 under high vacuum and at an operating voltage of 5 kV.
134
135   *2.6 Rheological measurements of PL/CS and GSH-PL/CS hydrogels*
136   Rheological measurements of PL/CS and GSH-PL/CS hydrogels were performed on a rotational
137 rheometer at oscillation modus (Kinexus Lab, Malvern Instruments Ltd) with a parallel plate (PP)
138 geometry (diameter 70 mm, angle 2.576 rad and gap between the plates of 1.02 mm) and a Peltier
139 temperature-controlled holder. For determination of elastic (G') and loss (G'') moduli, a volume of 1
140 mL of each hydrogel sample were transferred to the rheometer. A temperature ramp was applied
141 from 10 to 50°C at a heating rate of 5.0°C·min-1, with a fixed frequency of 1.0 Hz and a shear stress of
142 2.0 pA. The temperature when G' > G'', and the sample demonstrated a solid-like gel formation, was
143 related to gelling temperature (T_{gel}). Each experiment was repeated twice and analyzed using rSpace
144 software. In a further step, the temperature was fixed at 32.5°C and the frequency was varied from
145 0.1 to 10 Hz in order to evaluate the stability of the hydrogel. Each experiment was repeated twice
146 and analyzed using rSpace software.
147
148
149   *2.7 Thermal analyses of PL/CS and GSH-PL/CS hydrogels*
150   Thermal characterization of the PL/CS and GSH-PL/CS hydrogels was performed by
151 Differential Scanning Calorimetry (DSC) employing the DSC Q200 (TA) (DE, USA) equipment. The
152 reference in all cases was a standard aluminum sample holder. Samples of 0.2 mL of PL/CS or
153 GSH-PL/CS hydrogel were analyzed using heating-cooling cycles in the range of 0–65°C, with a
154 heating rate of 5°C·min-1, employing nitrogen to purge the gas chamber (50 mL·min-1). The cycles
155 were as follows: cycle 1 cooled from 25ºC to -10ºC, cycle 2 heated from -15ºC to 65ºC, cycle 3 cooled
156 from 65ºC to -15ºC and cycle 4 heated from -15ºC to 65ºC. The data were analyzed using Universal
157 Analysis 2000 software (TA Instruments version 4.5A). The critical micellization temperature (CMT)
158 was determined from the endothermic peak in the recorded DSC thermographs, and the enthalpy
159 change (ΔH) of the endothermic peak was calculated.
160
161   *2.8 Kinetics of NO release*
162   Kinetics of NO release from aqueous GSNO and from GSNO-containing hydrogel
163 (GSNO-PL/CS) were monitored by measuring changes in absorbance intensity at 545 nm (nN→π*
164 transition), by using the UV-visible spectrophotometer (Agilent 8454, Palo Alto, CA, USA), with a
165 temperature-controlled sample holder. Changes at 545 nm are solely associated with S-N bond
166 cleavage and free NO release [33,34,39]. Kinetic data were acquired at temperatures of 25, 32.5 and
167 37ºC. The initial concentration of GSNO in all groups was 50 mmol·L-1. The quantity of NO released
168 over time was calculated following Eqns. 1 and 2 [22, 40]. The results were reported as the mean ±
169 standard deviation (SD) of three independent experiments and expressed in terms of the NO
170 concentration:
171

$$[NO]t = [GSNO]_0 - [GSNO]_t \qquad\qquad\qquad\qquad\qquad\qquad (1)$$

$$[NO]t = \frac{A_0 b}{\varepsilon GSNO} - \frac{A_t b}{\varepsilon GSNO} \qquad . \qquad\qquad\qquad\qquad (2)$$

172
173   Equations 1 and 2 relate NO concentration at time, t, ([NO]t) to the GSNO absorption band,
174 wherein [GSNO]0 and [GSNO]t are the concentrations of GSNO at the beginning of the reaction and
175 at time, t, respectively. Variables A0 and At are the GSNO absorbances, at 545 nm, at the beginning
176 of the monitoring and at time, t, respectively. Variable εGSNO is the molar absorption coefficient of
177 GSNO at 545 nm (equals to 18.4 mol-1·L·cm-1), and b is the optical path of cuvette, which
178 corresponds to 1 cm.

179
180   *2.9 In vitro GSNO diffusion*
181   The in vitro kinetics of intact GSNO diffusion from aqueous GSNO and from GSNO-containing
182 hydrogel (GSNO-PL/CS) were carried out by using a vertical diffusion cell (standard cell, 15 mm of
183 diameter, 7 mL, Hanson Research Corporation) [41]. The cell consisted of donor and receptor
184 chambers, separated by polysulfone membrane disc filters with a 450 nm pore size (Tuffryn, Pall
185 Corporation, Port Washington, NY, USA). The donor compartment was filled with 2.5 mL aqueous
186 GSNO (GSNO in PBS) or GSNO-PL/CS hydrogel, in which the initial GSNO concentration was 50
187 mmol·L^{-1}, in both cases. The receptor compartment was filled with PBS, kept under magnetic stirring
188 at 32.5 ± 0.5ºC and the entire cell was protected from ambient light. A volume of 500 µL was
189 withdrawn from the receptor compartment, in 30 min intervals, and replaced by an equivalent
190 volume of fresh PBS solution. The withdrawn samples were immediately analyzed by UV-visible
191 spectrophotometry. The amount of intact GSNO diffused through the membrane was determined by
192 monitoring the spectral changes at 336 nm (ε = 980 mol-1·L·cm-1), and assigned to the presence of
193 intact GSNO [33,34,40]. The results were reported as the mean ± standard deviation (SD) of three
194 independent experiments and expressed in terms of the GSNO percentage.
195
196   *2.10 Mathematical models*
197   In order to investigate the mechanism of GSNO diffusion from the PL/CS hydrogel, the Higuchi
198 mathematical model was applied to the kinetic curve obtained in item 2.9 (Eq. 3) [42]:

        Qt= K$_H$ t$^{0.5}$ (3)

199   where Qt is the cumulative amount of drug released at time, t, KH is the release constant, and t is the
200 time [33,43, 44].
201
202   *2.11 Cytotoxicity of CS/PL and GSNO-PL/CS hydrogels*
203   The cytotoxicity effects of CS/PL and GSNO-CS/PL hydrogels were evaluated towards
204 Vero cells by MTT—3-(4,5-dimethylthiazol-2-yl)-2,5-diphenyltetrazolium bromide) assay [45,46].
205 Vero cells passage 173 (CCIAL-057) were seeded in 24-well plates. After 24 h, at a confluence of 80%
206 and after forming a monolayer, the culture medium was removed and substituted by elution
207 medium, prepared using cell culture medium and the hydrogels. The hydrogels were added to each
208 well containing Vero cells at concentrations of 0.2, 1.2, 2.4, 6.0 and 9.5 µg·mL^{-1} of PL/CS hydrogel.
209 These concentrations correspond to 0.2, 1.2, 2.4, 6.0 and 9.5 mmol·L^{-1} of GSNO, respectively (final
210 concentrations). After adding each formulation to Vero cells, they were incubated for 24 h at 37°C in
211 a 5% CO2 atmosphere. The pure culture medium was employed as a negative control, and a solution
212 of phenol (0.25%) was used as a positive control (cytotoxic) [47-49]. After Vero cell incubation for 24
213 h with the PL/CS hydrogel and GSNO-PL/CS hydrogel, a volume of 100 µL of 10% MTT solution (5
214 mg·mL^{-1}) in PBS was added to each of the wells, and the cells were incubated for an additional 4 h.
215 After removing MTT solution, 50 µL of dimethyl sulfoxide was added to each well for 10 min, and
216 the absorbance at 570 nm was measured with an automated spectrophotometric microtiter plate
217 reader (SpectraMax M5). The experiment was performed in triplicate. The results were presented as
218 the mean ± standard deviation (SD). The ANOVA test (one-way) was done, followed by the post hoc
219 Tukey test for comparison between the two groups. Statistical significance was set at a p-value of ≤
220 0.001.
221
222   *2.12 Morphological evaluation of Vero cells after treatment with the hydrogels*
223   The morphology of Vero cells after 24 h incubation with pure PL/CS or GSNO-PL/CS hydrogels
224 (at final hydrogel concentration of 0.2 – 9.5 µg·mL^{-1}) was observed with an inverted microscope
225 (AxioVert A1, Zeiss) and phase contrast [49,50].
226

227   *2.13 Antibacterial activity of PL/CS and GSNO-PL/CS hydrogels*

228   The minimal inhibitory concentration (MIC) and minimal bactericidal concentration (MBC) of
229   the PL/CS and GSNO-PL/CS hydrogels were carried out by microdilution assay, as described by the
230   Clinical and Laboratory Standards Institute [51]. The bacterial strain evaluated was the
231   gram-negative (standard CLSI) *Pseudomonas aeruginosa* ATCC 27853 (PAR). Initially, the bacteria
232   were grown in Mueller–Hinton solid medium at 37ºC to obtain the isolated colonies. Subsequently,
233   the colonies were solubilized in a saline solution 0.85% (w/v) and adjusted to the 0.5 index of the
234   MacFarland scale (1.5×10^8 colony-forming units (cfu) per mL). This solution was diluted in
235   Mueller–Hinton broth and distributed in a 96-well plate at a density of 10^6 cfu/well. Each well was
236   treated with different concentrations of PL/CS and GSNO-PL/CS hydrogels of 0.3, 0.5, 1.0, 2.1, 3.15
237   and 4.2 $\mu g \cdot ml^{-1}$, which correspond to NO final concentrations of 0.5, 1.0, 2.0, 4.0, 6.0 and 8.0 mmol$\cdot L^{-1}$,
238   respectively. The plates were incubated for 18 h and the bacterial growth was measured after this
239   period. The MBC tests were performed after the MIC tests. After 24 h of incubation, drops of
240   bacterial broth from the cavity with no visual growth were added to a Petri dish with the
241   Mueller-Hinton solid medium, and bacterial growth was observed after 48 h. These tests were
242   carried out in triplicate.

3. Results

244   Hydrogels are three-dimensional polymeric networks (Figure 1) with a soft consistency, high
245   porosity and water content [24, 31, 52]. Biocompatible hydrogels might simulate living tissues more
246   than any other class of synthetic biomaterial, due to their similarities [31,52]. They are easy to apply
247   into several shapes and surfaces because of their softness. Thus, they are predominantly used in
248   biomedical and topical applications [31].

249   Pluronics (Sigma) or Poloxamer (Bayer) are co-polymers largely used for hydrogel preparation
250   [53]. They are made of poly (ethylene oxide)-poly (propylene oxide)-poly (ethylene oxide)
251   (PEO-PPO-PEO) units. PPO segments are more hydrophobic, whereas PEO is more hydrophilic [21,
252   23]. There are several types of Pluronics, depending on the number of PEO and PPO units [23]. In
253   this study, we used the Pluronic F-127 (PL) with 106 units of PEO and 70 units of PPO [23].

254   In aqueous environments, PL chains undergo a spontaneous self-organization due to the
255   differences is solubility between PEO and PPO units, leading to the formation of micelles
256   (micellization process) [23]. The PPO segment of PL is comprised of the hydrophobic core of the
257   micelles, whereas the PEO segment of PL is comprised a hydrophilic shell [21]. The gelation process
258   determines the space organization of the micelles (hexagonal, cubic or lamellar phases) [23]. Upon
259   an increase in the temperature and/or PL concentration, micelles auto assemble, leading to a
260   three-dimensional polymeric network, as illustrated in Figure 1 [23]. The gelation process leads to an
261   increase in the viscosity of the polymer solution, leading to a gel state [23]. The Pluronic systems are
262   thermosensitive, which means they exist as liquids at low temperatures and become semi-solid at
263   higher temperatures. This phenome is reversible [21, 23]. Due to these properties, it is possible to
264   incorporate either hydrophilic [22, 40, 49, 54] or hydrophobic drugs into PL hydrogels [55].

265   The CS based biomaterials have gained a lot of attention due to their biocompatibility,
266   biodegradability and hemostatic properties for drug delivery and tissue engineering [38, 56-58]. The
267   interaction of positive protonated CS amino groups with the negatively charged mucin layer and
268   tight junctions can facilitate the transport of hydrophilic macromolecules through the mucosal
269   barrier [59]. In this present work, a NO-releasing hydrogel was prepared by incorporating the NO
270   donor (GSNO) into a PL/CS hydrogel. Both PL and CS are biocompatible polymers extensively
271   employed in medical applications. PL is responsive to forming the hydrogel network. This matrix
272   permits an easy topical application allowing a site-specific release of the NO donor/NO. The
273   presence of CS into the hydrogel matrix provides advantages due to its muco-adhesiveness
274   characteristic over commercial formulations [53]. In addition, CS is a well-known antimicrobial
275   biopolymer extensively used in biomedical and pharmaceutical applications [27]. In biological
276   systems, at low concentrations, GSNO has regulatory effects (promotion of tissue regeneration,
277   wound healing and vasodilation), whereas at high concentrations it has antimicrobial effects [3, 60].

278   Therefore, all of these combined properties can compose a versatile and suitable material for drug
279   delivery of NO in topical applications. To the best of our knowledge, this is the first paper to
280   describe the preparation and characterization of NO releasing PL/CS hydrogel with biocompatibility
281   and antibacterial effect.
282
283   *3.1. Characterization of PL/CS and GSH-PL/CS hydrogels*
284   In this study, GSH is the precursor of the NO donor molecule, GSNO. Due to the intrinsic
285   thermal and photochemical instability of GSNO [7, 22, 40], the characterization of morphological,
286   rheological and thermal properties of the hydrogel was performed with the GSH-PL/CS hydrogel.
287   The morphology of PL/CS and GSH-PL/CS hydrogels was observed by SEM analyses of lyophilized
288   formulations [24, 37]. Figure 2(a) exhibits a representative image of the PL/CS hydrogel. A smooth
289   surface with defined edges and amorphous structures can be observed. Figure 2(b) exhibits a
290   representative image of the GSH-PL/CS hydrogel. The GSH incorporation into the hydrogel leads to
291   a more irregular surface. It should be noted that dynamic surfaces, as observed in Figure 2(b), might
292   increase cell adhesion, migration and detachment, which is desirable for tissue engineering
293   applications [61]. The hydrogels studied here have similar morphologies to those described by
294   Leyva-Gomes et al., who characterized PL and PL/CS hydrogels prepared by gamma irradiation
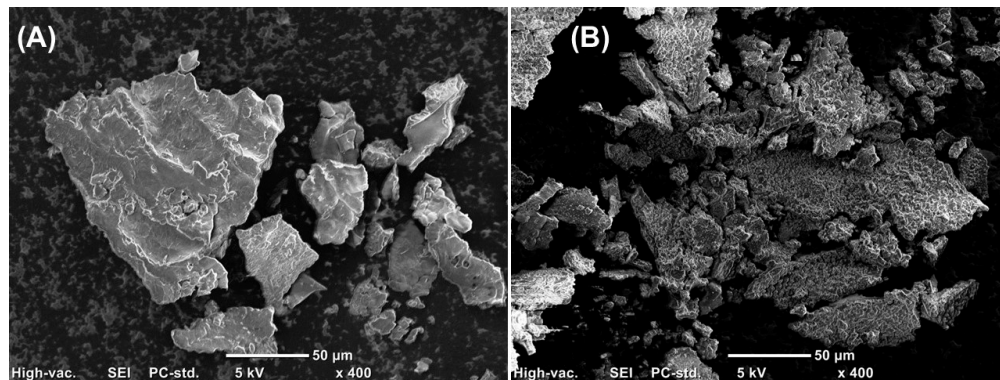295   [37].
296

Figure 2. Scanning electron microscopy (SEM) micrographs of lyophilized (A) PL/CS hydrogel and
(B) GSH-PL/CS hydrogel, using a 400x of magnification. The scale bar represents 50 μm.

300   Due to the presence of PL into the hydrogels, PL/CS and GSH-PL/CS hydrogels became
301   thermoresponsive hydrogels [62]. At low temperatures (0-5ºC), PL/CS and GSH-PL/CS hydrogels
302   had viscous behavior, whereas at higher temperatures (20 - 40°C) the hydrogel had a solid-like
303   behavior [62]. The gelling temperature (T_{gel}) indicated the temperature required to change the
304   rheological property of the material, and is understood as when elastic modulus (G′) becomes higher
305   than loss modulus (G″) during a temperature ramp [63]. This feature can be related to the presence
306   of PL into the hydrogel matrix, and has attracted significant interest involving drug release
307   applications and tissue engineering [64].
308   T_{gel} values of PL/CS and GSH-PL/CS hydrogels were found to be 28.72 ± 0.98°C and 29.95 ±
309   0.85°C, respectively (Table 1). The GSH incorporation on the PL/CS hydrogel slightly increased T_{gel}
310   by 1ºC. Kkatheb et al. showed a similar result upon the addition of laxacin into PL hydrogel, where
311   their results showed an increase of T_{gel} approximately of 1ºC [65].
312   Oscillation sweep frequency tests were performed on PL/CS and GSH-PL/CS hydrogels at
313   32.5ºC (the skin temperature) to evaluate the effect of GSH incorporation under the linear
314   viscoelastic region [64]. Figure 3(a) shows that the G′ and G″ moduli did not significantly change in
315   the applied frequency range (0.1-10 Hz). In addition, there was a linear region with a similar profile
316   for PL/CS and GSH-PL/CS hydrogels for all tested frequencies (Figure 3(a)). Thus, the GSH
317   incorporation into PL/CS hydrogel did not significantly change the hydrogel mechanical and gelling
318   properties.
319

Table 1. T_{onset} (°C), critical micellar temperature (CMT) (°C), T_{endset} (°C) and $\Delta H(J \cdot g^{-1})$ acquired using DSC analyses and $T_{sol/gel}$ (°C) acquired using rheology analyses of PL/CS and GSH-PL/CS hydrogels.

Material	T_{onset} (°C)	CMT(°C)	T_{endset} (°C)	$\Delta H(J \cdot g^{-1})$	T_{gel} (°C)
PL/CS	12.71	16.15	19.48	4.013	28.72 ± 0.98
GSH-PL/CS	6.57	10.69	14.75	4.237	29.95 ± 0.85

Figure 3. (A) Elastic (G′) and loss (G″) moduli of PL/CS hydrogel (black line) and GSH-PL/CS hydrogel (blue line) during an oscillation sweep frequency test at 32.5ºC. (B) Differential scanning calorimetric (DSC) thermographs of PL/CS hydrogel (black line) and GSH-PL/CS hydrogel (blue line).

DSC is an important technique to evaluate the temperature that induces thermal transitions in solutions of thermoresponsive polymers [65]. Figure 3(b) exhibits the thermographs of PL/CS and GSH-PL/CS hydrogels, with the aim to investigate thermal transition changes after GSH incorporation. The PL/CS hydrogel showed an endotherm peak with an onset temperature (T_{onset}) at 12.71°C, a peak at 16.15°C and an end set temperature (T_{endset}) of 19.48°C (Table 1). The endotherm peak can be related to the critical micellization temperature (CMT) process. In addition, T_{onset} is mainly related to the beginning of micelle formation, whereas T_{endset} shows the completion of the micelle formation process [65]. The incorporation of GSH into the PL/CS hydrogel decreased the T_{onset} by 6.14°C, CMC by 5.46ºC and T_{endset} by 4.73ºC (Figure 3(b) and Table 1). Thus, the GSH incorporation decreased the CMT by 40%. The micelle formation process is related to the dehydration of PPO block units in PL structure. The incorporation of GSH (hydrophilic molecule) is expected to form into a hydrophilic layer of the micelle, so the presence of GSH caused the dehydration of PPO block and, consequently, decreased the CMT value. The same trend was observed by Nie et al. by adding paclitaxel into PL hydrogel [22, 42].

Enthalpy variation (ΔH) is the area under the endothermic peak related to CMC. The ΔH values of PL/CS hydrogel and GSH-PL/CS hydrogel were found to be 4.013 and 4.237 J·g-1, respectively (Table 1). All formulations showed a positive ΔH. This result is related to the dehydration of the PPO block, which is an endothermic process. Thus, GSH incorporation into PL/CS hydrogel increased the ΔH value by 10%. Akkari et al. have shown a similar behavior by adding budesonide to PL hydrogels [66].

Taking together, the morphological, rheological and thermal properties of the GSH-PL/CS hydrogel were found to be suitable for drug delivery, since thermoresponsive behavior and desirable stability against oscillation were observed. These combined features make this hydrogel a potential candidate for topical applications of active molecules, such as NO/NO donors [31].

3.2. NO release from GSNO-PL/CS hydrogel

GSH is the precursor molecule of the NO donor, GSNO. In this work, GSH was nitrosated by reacting with an equimolar amount of NaNO2, in acid medium, forming the GSNO (Eq. 4). In this case, the nitrosating agent was nitrous acid (HNO2), which is formed by the dissolution of NO2- in aqueous acidified solution.   Once synthesized, GSNO was incorporated into PL/CS hydrogel:

$$GSH + HNO_2 \rightarrow GSNO + H_2O. \hspace{3cm} (4)$$

In this work, the kinetics of NO release from GSNO (either dissolved in aqueous solution or incorporated into GSNO-PL/CS hydrogel) was monitored for 24 h, at different temperatures. GSNO undergoes to a spontaneous decomposition releasing free NO and yielding oxidized glutathione (GSSG) (Eq. 5) [1, 9,22,33]:

$$2\ GSNO \rightarrow 2\ NO + GSSG. \hspace{3cm} (5)$$

This reaction occurs through the homolytic cleavage of S-N bond, which can be catalyzed by the presence of metal ions (e.g. copper), light and heat (1, 9, 22, 33).
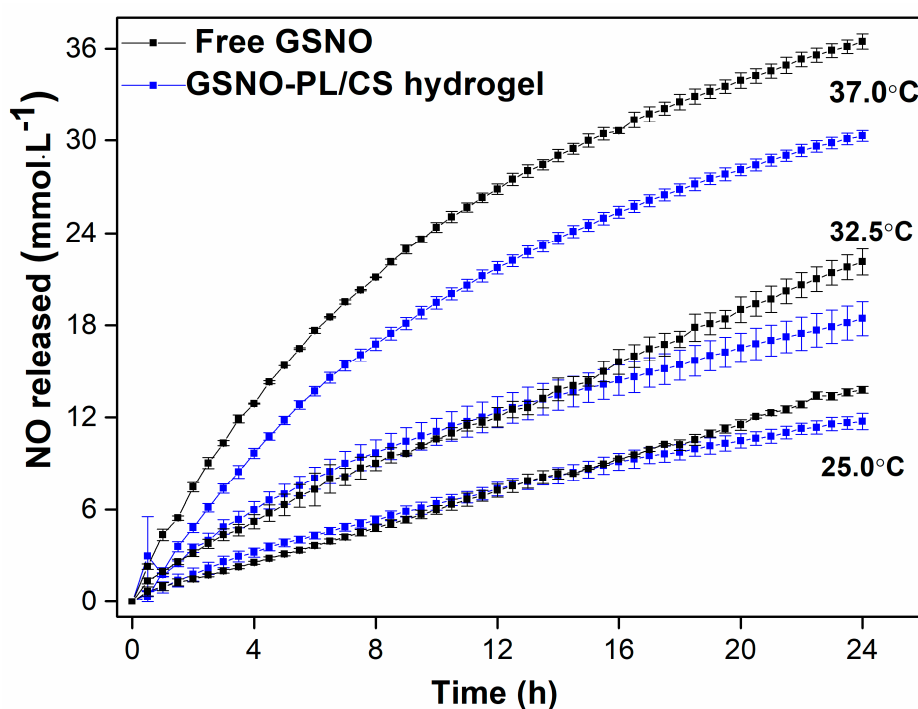

Figure 4. Kinetics of NO release from GSNO (initial concentration of 50 mmol·L^{-1}) in aqueous solution (black lines) and incorporated into PL/CS hydrogel (blue lines), at 25, 32.5 and 37°C.

Figure 4 shows the NO release profile from free GSNO and from GSNO-PL/CS hydrogel at different temperatures (25, 32.5 and 37ºC) for 24 h. As the stability of GSNO is known to be dependent on the temperature [39], the NO release profile was monitored at room, skin and physiological temperatures (25, 32.5 and 37°C, respectively). Figure 4 shows that both GSNO in aqueous solution, and GSNO incorporated into the hydrogel matrix, were able to release NO for at least 24 h at the different tested temperatures. In addition, the increase of the temperature increased the rates of NO release from both aqueous GSNO and hydrogel containing GSNO. This result is in accordance with previous publications [7, 9, 22, 30].

383   Furthermore, the incorporation of GSNO into PL/CS hydrogel decreased the rates of NO
384   release, compared to GSNO dissolved in aqueous solution (Figure 4), as previously reported when
385   complexed to other materials [9, 20, 54]. This decrease was assigned to the cage effect promoted by
386   the higher viscosity of the hydrogel matrix, in comparison to the aqueous environment. The superior
387   viscosity of the hydrogel matrix favors the radical pair recombination of NO• and GS•, restoring the
388   GSNO molecule, and increasing the rates of NO release. In this sense, the viscosity of the medium
389   can be used to modulate the rates of GSNO decomposition, and consequently the rates of NO release
390   [31].
391   Figure 4 shows that the concentration of NO release from GSNO was in the millimolar range. At
392   this range, NO is expected to have therapeutic effects [60], such as antibacterial activity. After 24 h at
393   37ºC, the total concentration of NO release from aqueous GSNO was ca. 36 mmol·L^{-1}, while the
394   concentration of NO release from the hydrogel was 30 mmol·L^{-1} (Figure 4). The incorporation of
395   GSNO into the PL/CS hydrogel decreased the amount of total NO released by 20%, at the same
396   period of time.
397   It should be noted that for therapeutic purposes, a sustained and localized release of NO is
398   desirable. Figure 4 shows that the incorporation of GSNO into PL/CS hydrogel promotes a sustained
399   NO release, in concentrations suitable for biomedical applications, for at least 24 h, at physiological
400   and skin temperatures. In addition, the hydrogel allows an increase in residence time of the NO
401   donor directly on the target site of application, making this formation good candidate for topical NO
402   delivery system [1, 7, 67-69].
403
404   *3.3. GSNO release from GSNO-PL/CS hydrogel*
405   The vertical Franz diffusion cell was used to evaluate the diffusion of intact GSNO through a
406   membrane versus GSNO dissolved in aqueous solution and GSNO-PL/CS hydrogel, at 32.5°C (skin
407   temperature). Figure 5 shows that in both cases, a two-phase release profile of GSNO was observed,
408   which included: (1) an initial burst of GSNO diffusion (within the first 1.5 h of monitoring), and (2)
409   the establishment of a plateau, which corresponded to a steady-state of GSNO diffusion release [20,
410   70]. This diffusion profile is similar to other reports published by the authors [30,32,33].
411   Additionally, Wu et al. showed a similar GSNO release profile from free GSNO and GSNO
412   encapsulated into polymer nanocomposite particles [71].
413   The diffusion of GSNO from aqueous GSNO reached a value of 50% of the total GSNO content
414   after 4.5 h of monitoring, whereas in the case of GSNO-PL/CS hydrogel the amount of GSNO that
415   diffused was 20%, at the same time frame (Figure 5). Indeed, the incorporation of GSNO into the
416   PL/CS hydrogel decreased the amount that GSNO diffused by 60%. This result is in accordance with
417   Figure 4 (i.e. kinetics of NO release from aqueous and GSNO-containing hydrogel). The superior
418   viscosity of the hydrogel matrix, related to the aqueous solution, promotes sustained and controlled
419   GSNO diffusion from the hydrogel matrix, making this formulation suitable for topical applications.
420   The Higuchi mathematical model was fit to the data presented in Figure 5 with a correlation
421   coefficient (R^2) of 0.991. This indicates a Fickian diffusion of GSNO from GSNO-PL/CS hydrogel
422   with a constant (KH) of 9.439 % h-1. Similar studies involving S-nitrosothiols showed a release
423   mechanism mainly limited by the Fickian diffusion. For example, Oliveira et al. showed the Fickian
424   release of NO from chitosan nanoparticles for agriculture applications [39], and Pelegrino et al.
425   showed a Fickian diffusion of GSNO from pure PL hydrogels or from hydrogel containing chitosan
426   nanoparticles [32]. Therefore, GSNO incorporation into the PL/CS hydrogel significantly decreased
427   the rates GSNO diffusion from the hydrogel matrix, allowing a sustained release of the NO donor
428   directly onto the desired site of application.
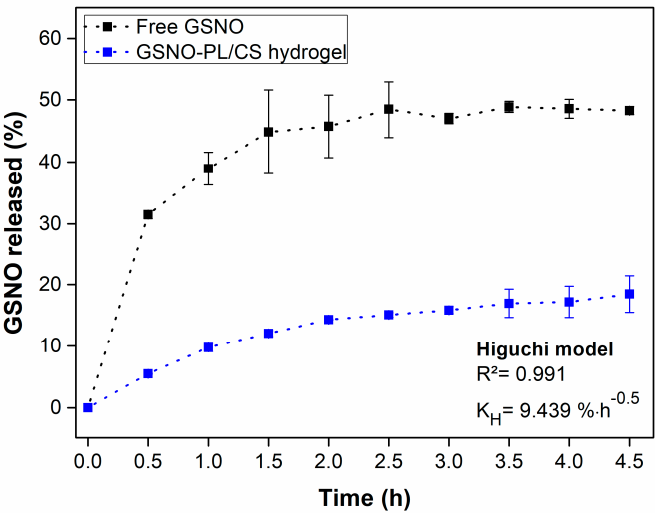429
430
431

432

Figure 5. In vitro release profile of free GSNO (black line) and GSNO-PL/CS hydrogel (blue line), using a Franz diffusion cell system at 32.5ºC (initial GSNO concentration of 50 mmol·L^{-1}).

3.4. Cytotoxicity of PL/CS and GSNO-PL/CS hydrogels

The biocompatibility of the GSNO-PL/CS hydrogel was accessed as an in vitro cytotoxicity test using Vero cells, a lineage mentioned at the ISO 10993-5 [47] standard for these tests. These adherent cells show fibroblastic morphology and express cytotoxicity results in contact with different biomaterials and solutions [72-74].

Cytotoxicity assays were performed by varying concentrations of the PL/CS and GSNO-PL/CS hydrogels. Namely, 0.2, 1.2, 2.4, 6.0 and 9.5 µg·mL^{-1} of PL/CS hydrogel were used, and these concentrations correspond to 0.2, 1.2, 2.4, 6.0 and 9.5 mmol·L^{-1} of GSNO, respectively (in the case of GSNO-containing hydrogel). Cytotoxicity was assessed by MTT assay, using the Vero cell line, and by morphological cell characterization after cell incubation with the hydrogels for 24 h.

Figure 6 shows that both hydrogels showed a concentration-related cytotoxicity. For the PL/CS hydrogel, concentrations under 2.4 µg·mL^{-1} were considered noncytotoxic. However, in the presence of GSNO-containing hydrogel, the cytotoxicity of the formulation towards Vero cells was observed at concentrations under 1.2 µg·mL^{-1}. As expected, the hydrogels did not significantly decrease cell viability at lower concentrations. A decrease in cell viability was found for the higher tested concentrations.
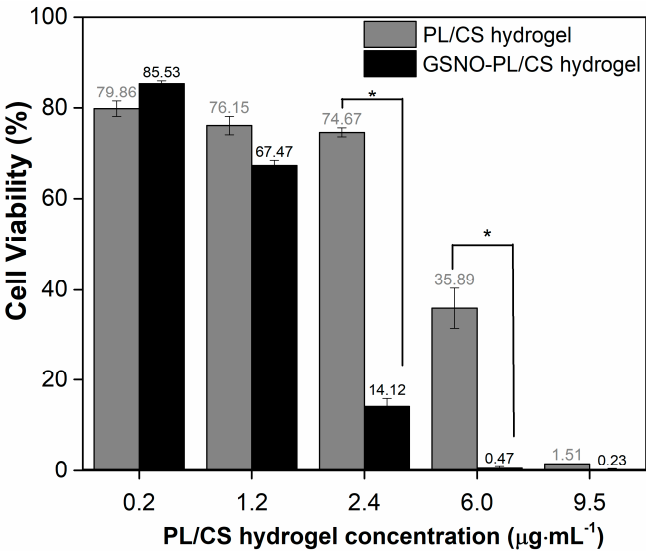
451

452

453

454

Figure 6. Vero cell viability after incubation with PL/CS and GSNO-PL/CS hydrogels (at final hydrogel concentrations of 0.2 – 9.5 µg·mL⁻¹) for 24 h.

The cytotoxic pattern is shown in Figures 7(a) to (f). Noncytotoxic Vero cells grew in a confluent monolayer, with a fibroblastic-like polygonal morphology (Figure 7(g)). With the presence of a cytotoxic compound, namely 0.25 % phenol, the cell showed a rounded and loose morphology, non-attached, and lifted from the culture plates, with signs of cell death (Figure 7(h)). These parameters were used to analyze the different tested compounds, PL/CS and GSNO-PL/CS hydrogel.
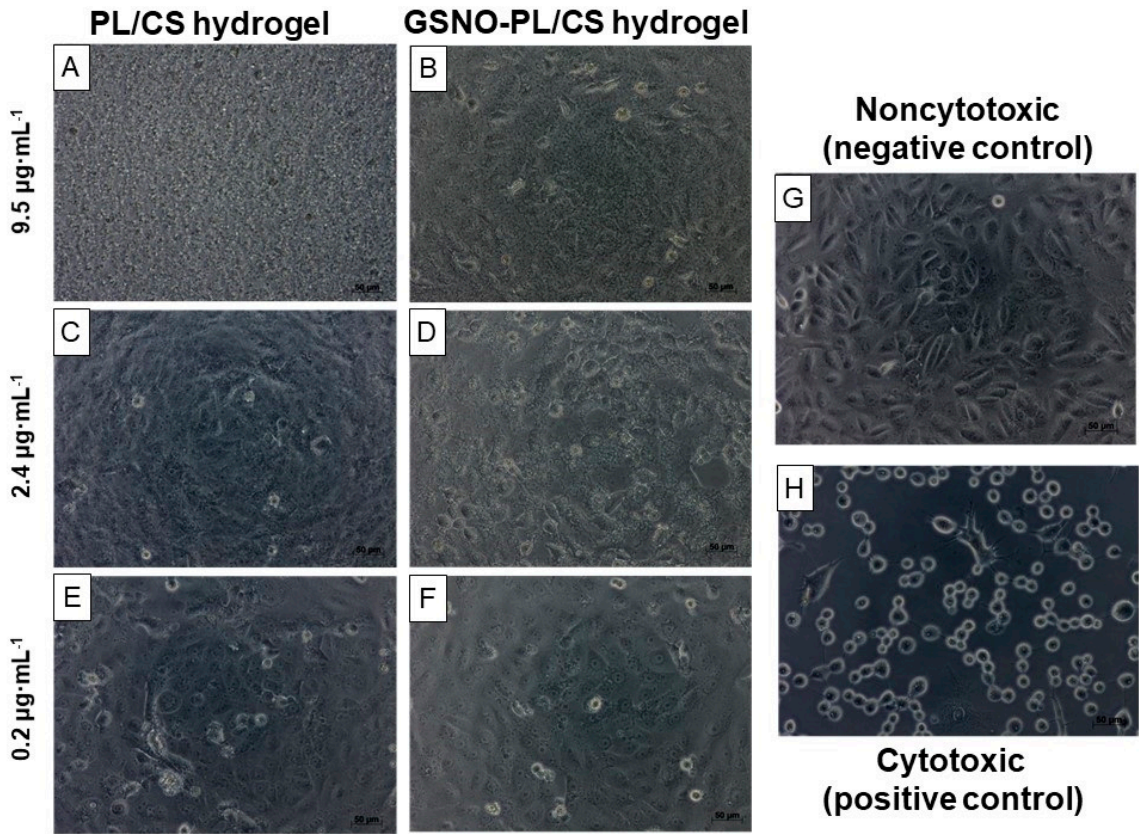

Figure 7. Morphological characterization of Vero cells incubated with PL/CS hydrogel (first column) and GSNO-PL/CS hydrogel (second column) at 9.5 µg·mL⁻¹ (A and B, respectively), 2.4 µg·mL⁻¹ (C and D, respectively) and 0.24 µg·mL⁻¹ (E and F, respectively) for 24 h. Control samples (third column) of non-cytotoxicity (G) and cytotoxicity (H).

The predominance of the PL/CS-hydrogel can be observed in Figures 7(a) and (b), which consequently covered and/or caused the death of Vero cells. With the decrease in the concentration of the tested components, the presence of the cells, and morphology similar to the non-cytotoxic control, were observed (Figs. 7(c) to (f)).

At hydrogel concentrations higher than 1.2 µg·mL⁻¹, the presence of rounded and debris cells can be observed, a typical characteristic of cytotoxicity (Figs. 7(b) and (d)). These results demonstrated a concentration-dependent cytotoxicity of the GSNO-PL/CS hydrogel to the Vero cell line. These data are in accordance with a previous publication by the authors, which demonstrated that high NO levels are cytotoxic to different normal and cancerous cell lines [33,75]. These findings are also in agreement with several publications that demonstrated a concentration-dependence toxicity of different classes of NO donors towards health and tumor cell lines [33, 60, 76-78].

The proposed mechanisms of cytotoxicity caused by the NO donors involves the multifunctional transcription factor NF-κB, inhibition of both ribonucleotide reductase and ATP, or protein expression mediators [33, 76, 78]. Ferraz et al. studied the cytotoxicity mechanism of S-nitrosothiol-containing polymeric nanoparticle (NO-NP) against a melanoma cell line [75]. The

483 NO-NP induced apoptosis against melanoma cells with the activation of effector caspase 3.
484 Additionally, an increase of oxidative stress in the cells incubated with NO-NP was observed, which
485 was related to an increase generation of a superoxide anion radical by mitochondria [75].
486 In contrast, low concentrations of both hydrogels were not toxic to Vero cells (Figure 6). The
487 biocompatibility of systems composed of PL/CS hydrogels has been demonstrated through various
488 applications [24, 49, 79]. The thermosensitive response of the PL/CS hydrogel has been applied as an
489 injectable scaffold and as a cell delivery carrier matrix for tissue regeneration [36, 79-81]. Olguín et al.
490 reported advanced properties of this thermosensitive hydrogel for the delivery of cells in neural
491 tissue engineering, and demonstrated a delicate relationship between physical properties and
492 capabilities to promote cell proliferation and differentiation [79].
493 PL/CS hydrogels have also been applied as carrier systems for drug, gene and biomolecule
494 delivery [24, 82-86]. The common points of these studies was to combine and explore suitable
495 features of each polymer (PL and CS) in a single formation, i.e. mucoadhesion and thermogelling.
496 These were intended to prolong the residence time of the delivery systems, thus improving the
497 efficacy of local or systemic drugs/biomolecules [87]. Radivojša et al. developed a novel approach
498 based on thermoresponsive hydrogels with CS nanocomplexes for prolonged release of low
499 molecular weight heparins (LMWH). These double-responsive mixed preparations seemed to be
500 promising systems for subcutaneous LMWH delivery, requiring less frequent administration during
501 long-term treatment. Additionally, formulations demonstrated no cytotoxicity in vitro for human
502 keratinocyte cells [84]. The application of hydrogels as release systems for NO donor compounds has
503 also been described in the literature. De Oliveira (2016) developed a topical hydrogel formulation
504 comprising Pluronic F127 containing GSNO in concentrations ranging from 50 to 150 mmol·L^{-1} [39].
505 These formulations were shown to produce a significant dermal vasodilation in topical applications
506 on the healthy skin of volunteers [39, 40].

508 *3.5. Antibacterial activity of PL/CS and GSNO-PL/CS hydrogels*
509 The antimicrobial properties of PL/CS and GSNO-PL/CS hydrogels were investigated
510 against gram-negative bacteria, *Pseudomonas aeruginosa* (PAR). PAR is an important human
511 pathogen, responsible for a wide range of chronic and acute infections, such as diabetic foot
512 infections, burn wounds and pneumonia in cystic fibrosis patients [88-94]. PAR is particular resistant
513 bacteria against β-lactans antibiotics due to its intrinsic capability of expressing β-lactamases and
514 efflux pumps [91].
515 Both MIC and MBC values for PL/CS hydrogel were found to be 2.1 µg·mL^{-1}, whereas both MIC
516 and MBC values for GSNO-PL/CS hydrogel were found to be 0.5 µg·mL^{-1} (this concentration
517 corresponds to 1 mmol·L^{-1} of GSNO) (Table 2). The sole PL/CS hydrogel had a bacterial effect,
518 however the incorporation of GSNO into the hydrogel decreased both MIC and MBC values by four
519 times. Thus, as expected, the PL/CS hydrogel demonstrated antibacterial activity (due to the
520 presence of CS), and this activity was enhanced by GSNO incorporation into the hydrogel matrix.
521 Interesting, by comparing Table 2 and Figure 6, the hydrogel concentration required to achieve an
522 anti-bacterial effect was not found to be cytotoxic (as related to a cytotoxicity pattern in Vero cells).
523 Therefore, there is a concentration range that the GSNO-containing PL/CS hydrogel that can be
524 safely administered to the patient, without damaging mammalian cells, and with a promising
525 antibacterial effect.

526 **Table 2.** Values of MIC and MBC for PL/CS and GSNO-PL/CS hydrogels against Pseudomonas
527 aeruginosa (PAR) ATCC 27853, as model microorganism.

	Pseudomonas aeruginosa (PAR) ATCC 27853	
	MIC (µg·mL^{-1})	MBC (µg·mL^{-1})
PL/CS hydrogel	2.1	2.1
GSNO-PL/CS hydrogel	0.5	0.5

530 Similar to our results, Hetrick et al. showed a treatment composed of nitrosated proline as a NO
531 donor (PROLI/NO) against PAR. The treatment exhibited a MIC value of 2.5 mg·mL^{-1} [95]. Seabra et
532 al. demonstrated the antibacterial effects of NO-releasing polyester [10] and NO-releasing-AgNPs
533 towards different gram positive and negative bacteria strains [2].   Barraud et al. studied the effect of
534 NO donor, sodium nitroprusside (SNP), against PAR strains in planktonic and biofilm forms [96]. At
535 concentration of 5 μmol·L-1 of SNP, a decrease of 50% in the CFU of planktonic PAR was observed.
536 In addition, the authors observed that this effect was decreased when the NO treatment was
537 combined with a phosphodiesterases inhibitor. Thus, the possible antibacterial mechanism of NO is
538 related to phosphodiesterases, which contributes to a genetic network that modulates virulence and
539 biofilm formation and dispersion [96].

540 NO is known to have a potent and wield-ranged antimicrobial effect against both
541 gram-negative and gram-positive bacteria [60]. The main mechanism by which NO kills bacteria is
542 understood to involve nitrosative stress, which evolves the production of reactive nitrogen/oxygen
543 species. As the antibacterial effect of NO involves multiply pathways, bacteria have, thus far, not
544 been able to develop resistance towards NO [60].

545 CS is also known to have antibacterial effects [82,88]. The main antibacterial effects caused by
546 CS include: (1) cell penetration and interaction with DNA; (2) CS chelation of metal ions, which leads
547 to the production of toxins, inhibition of enzymatic activity, and finally the cell cycle and (3)
548 electrostatic interactions between positively charged CS and negatively charged cell membrane [88].

549 Thus, a biomaterial that combines the antimicrobial activities of CS and NO might be
550 considered a potent antimicrobial agent. In addition, the viscosity of the semi-solid hydrogel matrix
551 allows its topical/dermatological applications, increasing the contact time and, therefore, the
552 interaction of the formulation with application target sites. In this sense, the NO/NO donor can be
553 directly released from the hydrogel matrix. This approach might find important applications in the
554 treatment of skin and soft tissue infections, such as diabetic foot infections, otitis externa and burn
555 wounds [94].

5. Conclusions

557 This work described the preparation, characterization, NO/GSNO release profile,
558 biocompatibility and antibacterial effects of GSNO-containing PL/CS hydrogel. This hydrogel can be
559 considered as a promising system for NO delivery due to its biocompatibility, easy preparation,
560 ability to incorporate NO donors, ability to promote a sustained NO and GSNO release and
561 antibacterial effect. Their main features of the hydrogel include smooth morphology,
562 thermoresponsive behavior and good mechanical stability. In addition, this system is free of
563 crosslink agents, increasing the biocompatibility of the hydrogel, due to the absence of possible toxic
564 sub-products. The GSNO-PL/CS hydrogel was found to release therapeutic amounts of NO in a
565 sustainable manner. GSNO-containing PL/CS hydrogel was not toxic towards the Vero cell at
566 concentrations lower than 13.23 μg·mL^{-1}, which increases the safety aspect of this material.
567 GSNO-containing PL/CS hydrogel demonstrated antibacterial effects against *Pseudomonas*
568 *aeruginosa*, with MIC and MBC values of 0.5 μg·mL^{-1} (this concentration corresponds to 1 mmol·L^{-1} of
569 GSNO). Importantly, the antibacterial effect of the NO-releasing hydrogel was observed at
570 concentrations that were not toxic to the Vero cell.

575 **Author Contributions:** Milena T. Pelegrino, Bruna de Araujo Lima and Mônica H. M. do Nascimento
576 performed the experimental work and analyzed the data. Milena T. Pelegrino, Christiane B. Lombello, Marcelo
577 Brocchi and Amedea B. Seabra were responsible for analyzing the experimental data and writing the paper. All
578 authors approved the manuscript.

579 **Conflicts of Interest:** The authors declare no conflict of interest.

580   **References**

581   1.   Seabra, A. B.; Justo, G. Z.; Haddad, P. S. State of the art, challenges and perspectives in the design of nitric
582   oxide-releasing polymeric nanomaterials for biomedical applications. *Biotechnol. Adv.* **2015**, 33, 1370–1379.

583   2.   Seabra, A.B.; Elgueta, N.M.; Lima, B.A.; Pelegrino, M.T.; Brocchi, M.; Rubilar, O.; Durán, N. Antibacterial
584   activity of nitric oxide releasing silver nanoparticles. J. Phys. Conf. Ser. **2017**,   838,   012031.

585   3.   Iganarro, L.; Freeman, B. Nitric Oxide Biology and Pathobiology, 3rd Edition, 2017, Elsevier.

586   4.   Carpenter, A. W.; Schoenfisch, M. H. Nitric oxide release Part II. Therapeutic applications. *Chem. Soc. Rev.*
587   **2012**, *41*, 3742–52.

588   5.   Seabra, A.B.; da Silva, R.; de Souza, G. F. P.; de Oliveira, M.G. Antithrombogenic polynitrosated
589   polyester/poly(methyl methacrylate) blend for the coating of blood-contacting surfaces. *Artif. Organs*,
590   **2008**, *32*,   262-267.

591   6.   Ignarro, L. J.; Buga, G. M.; Wood, K. S.; Byrns, R. E.; Chaudhuri, G. Endothelium-derived relaxing factor
592   produced and released from artery and vein is nitric oxide. *Proc. Natl. Acad. Sci.* **1987**, *84*, 9265–9269.

593   7.   Seabra,   A.   B.;   Fitzpatrick,   A.;   Paul,   J.;   de   Oliveira,   M.   G.;   Weller,   R.   Topically   applied
594   S-nitrosothiol-containing hydrogels as experimental and pharmacological nitric oxide donors in human
595   skin. *Br. J. Dermatol.* **2004**, *151*, 977–983.

596   8.   Fukuto, J. M.; Carrington, S. J.; Tantillo, D. J.; Harrison, J. G.; Ignarro, L. J.; Freeman, B. A.; Chen, A.;
597   Wink, D. A. Small molecule signaling agents: The integrated chemistry and biochemistry of nitrogen
598   oxides, oxides of carbon, dioxygen, hydrogen sulfide, and their derived species. *Chem. Res. Toxicol.* **2012**,
599   *25*, 769–793.

600   9.   Brisbois, E. J.; Handa, H.; Major, T. C.; Bartlett, R. H.; Meyerhoff, M. E. Long-term nitric oxide release and
601   elevated   temperature   stability   with   S-nitroso-N-acetylpenicillamine   (SNAP)-doped   Elast-eon   E2As
602   polymer. *Biomaterials* **2013**, *34*, 6957–6966.

603   10.   Seabra, A.B.; Martins, D.; Simões, M.M.S.G.; da Silva, R.; Brocchi, M.; de Oliveira, M. G.   Antibacterial
604   nitric oxide-releasing polyester for the coating of blood-contacting artificial materials. *Artif. Organs*, **2010**,
605   *34*, E204-E214.

606   11.   Wo, Y.; Brisbois, E. J.; Bartlett, R. H.; Meyerhoff, M. E. Recent advances in thromboresistant and
607   antimicrobial polymers for biomedical applications: just say yes to nitric oxide (NO). *Biomater. Sci.* **2016**, *4*,
608   1161–83.

609   12.   Frank, S.; Kämpfer, H.; Wetzler, C.; Pfeilschifter, J. Nitric oxide drives skin repair: Novel functions of an
610   established mediator. *Kidney Int.* **2002**, *61*, 882–888.

611   13.   Georgii, J.L.; Amadeu, T.P.; Seabra, A.B.; de Oliveira, M.G.; Monte-Alto-Costa, A. Topical
612   S-nitrosoglutathione-releasing hydrogel improves healing of rat ischaemic wounds. *J. Tissue Eng. Regen.*
613   *Med.* **2011**, 2011 5:612-9.

614   14.   Huang, B.; Liu, M.; Zhou, C. Chitosan composite hydrogels reinforced with natural clay nanotubes.
615   *Carbohydr. Polym.* **2017**, *175*, 689–698.

616   15.   Li, Y.; Wang, X.; Wei, Y.; Tao, L. Chitosan-based self-healing hydrogel for bioapplications. *Chinese Chem.*
617   *Lett.* **2017**, 3–7.

618   16.   Vercelino, R.; Cunha, T. M.; Ferreira, E. S.; Cunha, F. Q.; Ferreira, S. H.; de Oliveira, M. G. Skin
619   vasodilation and analgesic effect of a topical nitric oxide-releasing hydrogel. *J. Mater. Sci. Mater. Med.*
620   **2013**, *24*, 2157–2169.

621   17.   Kellogg, D. L.; Liu, Y.; Kosiba, I. F.; O'Donnell, D. Role of nitric oxide in the vascular effects of local
622   warming of the skin in humans. *J. Appl. Physiol.* **1999**, *86*, 1185–1190.

623   18.   Miclescu, A.; Gordh, T. Nitric oxide and pain: "Something old, something new." *Acta Anaesthesiol. Scand.*
624   **2009**, *53*, 1107–1120.

625   19.   Laftah, W. A.; Hashim, S.; Ibrahim, A. N. Polymer hydrogels: A review. *Polym. Plast. Technol. Eng.* **2011**,
626   *50*, 1475–1486.

627   20.   Malli, S.; Bories, C.; Pradines, B.; Loiseau, P. M.; Ponchel, G.; Bouchemal, K. *In situ* forming pluronic
628   F127/chitosan hydrogel limits metronidazole transmucosal absorption. *Eur. J. Pharm. Biopharm.* **2017**, *112*,
629   143–147

630   21.   Akash, M. S. H.; Rehman, K. Recent progress in biomedical applications of pluronic (PF127):
631   Pharmaceutical perspectives. *J Control Release.* **2015**, 120-138.

632   22.   Shishido, S. M.; Seabra, A. B.; Loh, W.; de Oliveira, M. G. Thermal and photochemical nitric oxide release
633   from S-nitrosothiols incorporated in Pluronic F127 gel: Potential uses for local and controlled nitric oxide
634   release. *Biomaterials* **2003**, *24*, 3543–3553.

635   23.   de Araujo, D. R.; Oshiro, A.; da Silva, D. C.; Akkari, A. C.; de Mello, J. C.; Rodrigues, T. Poloxamers as
636   Drug-Delivery Systems:Physicochemical, Pharmaceutical, and Toxicological Aspects. In *Nanotoxicology:*
637   *Materials, Methodologies, and Assessments*; Durán, N.; Guterres, S. S.; Alves, O. L., Eds.; Springer Science &
638   Business Media, 2013; pp. 281–298.

639   24.   Yu, S.; Zhang, X.; Tan, G.; Tian, L.; Liu, D.; Liu, Y.; Yang, X.; Pan, W. A novel pH-induced thermosensitive
640   hydrogel composed of carboxymethyl chitosan and poloxamer cross-linked by glutaraldehyde for
641   ophthalmic drug delivery. *Carbohydr. Polym.* **2017**, *155*, 208–217.

642   25.   Zou, P.; Yang, X.; Wang, J.; Li, Y.; Yu, H.; Zhang, Y.; Liu, G. Advances in characterisation and biological
643   activities of chitosan and chitosan oligosaccharides. *Food Chem.* **2016**, *190*, 1174–1181.

644   26.   Divya, K.; Vijayan, S.; George, T. K.; Jisha, M. S. Antimicrobial properties of chitosan nanoparticles: Mode
645   of action and factors affecting activity. *Fibers Polym.* **2017**, *18*, 221–230.

646   27.   Seabra, A. B.; Pelegrino, M. T. Chitosan-based nanomaterials for skin regeneration. *AIMS Med. Sci.* **2017**,
647   *4*, 352–381.

648   28.   Fernandez, J. G.; Ingber, D. E. Bioinspired chitinous material solutions for environmental sustainability
649   and medicine. *Adv. Funct. Mater.* **2013**, *23*, 4454–4466.

650   29.   Schmolka, I. K. Artificial skin: Preparation and properties of Pluronic F-127 gels for treatment of burns. *J.*
651   *Biomed. Mater. Res.* **1972**, *6*, 571-582.

652   30.   Pelegrino, M. T.; de Araújo, D. R.; Seabra, A. B. S-nitrosoglutathione-containing chitosan nanoparticles
653   dispersed in Pluronic F-127 hydrogel: Potential uses in topical applications. *J. Drug Deliv. Sci. Technol.*
654   **2017**.

655   31.   Champeau, M.; Seabra, A. B.; de Oliveira, M. G. Hydrogels for topical nitric oxide delivery. In *Nitric oxide*
656   *donors: Novel biomedical applications and perspectives*; Seabra, A. B., Ed.; Elsevier, **2017**; 13, 313-330.

657   32.   Pelegrino, M. T.; Weller, R. B.; Chen, X.; Bernardes, J. S.; Seabra, A. B. Chitosan nanoparticles for nitric
658   oxide delivery in human skin. *Med. Chem. Commun.* **2017**, *38*, 606–615.

659   33.   Pelegrino, M. T.; Silva, L. C.; Watashi, C. M.; Haddad, P. S.; Rodrigues, T.; Seabra, A. B. Nitric
660   oxide-releasing nanoparticles: synthesis, characterization, and cytotoxicity to tumorigenic cells. *J.*
661   *Nanoparticle Res.* **2017**, *19*.

662   34.   Silveira, N. M.; Frungillo, L.; Marcos, F. C. C.; Pelegrino, M. T.; Miranda, M. T.; Seabra, A. B.; Salgado, I.;
663   Machado, E. C.; Ribeiro, R. V. Exogenous nitric oxide improves sugarcane growth and photosynthesis
664   under water deficit. *Planta* **2016**, 1–10.

665   35.   Chang, F. C., Tsao, C.T., Lin, A., Zhang, M., Levengood, S. L., Zhang, M. PEG-Chitosan hydrogel with

666   tunable stiffness for study of drug response of breast cancer cells. *Polymers.* **2016**, *8*, 112.

667   36.   Yap, L. S.; Yang, M. C. Evaluation of hydrogel composing of Pluronic F127 and carboxymethyl hexanoyl
668   chitosan as injectable scaffold for tissue engineering applications. *Colloids Surf. B* **2016**, *146*, 204–211.

669   37.   Leyva-Gómez, G.; Santillan-Reyes, E.; Lima, E.; Madrid-Martínez, A.; Krötzsch, E.; Quintanar-Guerrero,
670   D.; Garciadiego-Cázares, D.; Martínez-Jiménez, A.; Hernández Morales, M.; Ortega-Peña, S.;
671   Contreras-Figueroa, M. E.; Cortina-Ramírez, G. E.; Abarca-Buis, R. F. A novel hydrogel of poloxamer 407
672   and chitosan obtained by gamma irradiation exhibits physicochemical properties for wound
673   management. *Mater. Sci. Eng. C* **2017**, *74*, 36–46.

674   38.   Wu, T.; Huang, J.; Jiang, Y.; Hu, Y.; Ye, X.; Liu, D.; Chen, J. Formation of hydrogels based on
675   chitosan/alginate for the delivery of lysozyme and their antibacterial activity. *Food Chem.* **2018**, *240*, 361–
676   369.

677   39.   de Oliveira, M. G. S-Nitrosothiols as Platforms for Topical Nitric Oxide Delivery. *Basic Clin. Pharmacol.*
678   *Toxicol.* **2016**.

679   40.   Seabra, A. B.; de Oliveira, M. G. Poly(vinyl alcohol) and poly(vinyl pyrrolidone) blended films for local
680   nitric oxide release. *Biomaterials* **2004**, *25*, 3773–3782.

681   41.   Franz, T. J. Percutaneous absorption on the relevance of *in vitro* data. *J. Invest. Dermatol.* **1975**, *64*, 190–195.

682   42.   Nie, S.; Hsiao, W. L. W.; Pan, W.; Yang, Z. Thermoreversible pluronic F127-based hydrogel containing
683   liposomes for the controlled delivery of paclitaxel: *In vitro* drug release, cell cytotoxicity, and uptake
684   studies. *Int. J. Nanomedicine* **2011**, *6*, 151–166.

685   43.   Costa, P.; Lobo, J. M. Modeling and comparison of dissolution profiles. *Eur. J. Pharm. Sci.* **2001**, *13*, 123–
686   133.

687   44.   Oshiro, A.; Silva, D. C.; Mello, J. C.; Moraes, V. W. R. De; Cavalcanti, L. P.; Franco, M. K. K. D.;
688   Alkschbirs, M. I.; Fraceto, L. F.; Yokaichiya, F.; Rodrigues, T.; Araujo, D. R. Pluronics F-127/L-81 binary
689   hydrogels as drug-delivery systems: in fl uence of physicochemical aspects on release kinetics and
690   cytotoxicity. *Langmuir* **2014**, *30*, 13689–13698.

691   45.   Mosmann, T. Rapid colorimetric assay for cellular growth and survival: application to proliferation and
692   cytotoxicity assays. *J. Immunol. Meth.* **1983**, *65*, 55-63.

693   46.   Kirkpatrick, C.J.; Bittinger, F.; Wagner, M.; Köhler, H.; van Kooten, T.G.; Klein, C.L.; Otto, M. Current
694   trends in biocompatibility testing. *Proc. Inst. Mech. Eng. H* **1998**, *212*, 75-84.

695   47.   International Standards Organization. ISO 10993-5. Biological evaluation of medical devices - Part 5: Tests
696   for in vitro cytotoxicity. **2009**. 34p.

697   48.   Rogero, S. O.; Lugão A. B.; Íkeda, T. I.; Cruz, A. S. Teste *in vitro* de citotoxicidade: estudo comparativo
698   entre duas metodologias. *Mater. Res.* **2003**, *6*, 317-320.

699   49.   Nascimento, M. H. M.; Ferreira, M.; Malmonge, S. M.; Lombello, C. B. Evaluation of cell interaction with
700   polymeric biomaterials based on hyaluronic acid and chitosan. *J. Mater. Sci. Mater. Med.* **2017**, *28*, 5, 68.

701   50.   Lombello, C.B.; Malmonge, S.M.; Wada, M.L.F. PolyHEMA and polyHEMA-poly(MMA-co-AA) as
702   substrates for culturing cells. *J. Mater. Sci. Mater. Med.* **2000**, *11*, 541-546.

703   51.   CLSI (2015). Performance Standards for Antimicrobial Susceptibility Testing. Twenty-Fifth Informational
704   Supplement CLSI Document M100-S25. Wayne, PA: Clinical and Laboratory Standards Institute.

705   52.   Caló, E.; Khutoryanskiy, V. V. Biomedical applications of hydrogels: A review of patents and commercial
706   products. *Eur. Polym. J.* **2015**, *65*, 252–267

707   53.   Domínguez-Delgado, C. L.; Fuentes-Prado, E.; Escobar-Chávez, J. J.; Vidal-Romero, G.; Rodríguez-Crus, I.
708   M.; Díaz-Torres, R. Chitosan and Pluronic® F-127: Pharmaceutical applications. *In* Encyclopedia of

709   Biomedical Polymers and Polymeric Biomaterials. Taylor and Francis: New York, **2016**, 1513-1535.

710   54.   Schanuel, F. S.; Santos, K. S. R.; Monte-Alto-Costa, A.; de Oliveira, M. G. Combined nitric oxide-releasing
711   poly(vinyl alcohol) film/F127 hydrogel for accelerating wound healing. *Colloids Surf. B* **2015**, *130*, 182-191.

712   55.   Pellosi, D. S.; Moret, F.; Fraix, A.; Marino, N.; Maiolino, S.; Gaio, E.; Hioka, K.; Reddi, E.; Sortino, S.;
713   Quaglia F. Pluronic® P123/F127 mixed micelles delivering sorafenib and its combination with verteporfin
714   in cancer cells. *Int. J. Nanomedicine* **2016**,*11*, 4479–4494.

715   56.   Li, P.; Zhao, J.; Chen, Y.; Cheng, B.; Yu, Z.; Zhao, Y.; Yana, X.; Tonga, Z.; Jina, S. Preparation and
716   characterization of chitosan physical hydrogels with enhanced mechanical and antibacterial properties.
717   *Carbohydr. Polym.* **2017**, *157*, 1383-1392.

718   57.   Tan, H.; Chu, C. R.; Payne, K.; Marra, K. G. Injectable *in situ* forming biodegradable chitosan-hyaluronic
719   acid based hydrogels for cartilage tissue engineering. *Biomaterials* **2009**, 30, 2499-2506.

720   58.   Bernkop-Schnurch, A.; Dunnhaupt, S. Chitosan-based drug delivery systems. *Eur. J. Biopharm.* **2012**, *81*,
721   463–469.

722   59.   Bowman, K.; Leong, K. W. Chitosan nanoparticles for oral drug and gene delivery. *Int. J. Nanomedicine*
723   **2006,** *2*, 117–128.

724   60.   Seabra, A.B. Nitric oxide donors: Novel biomedical applications and perspectives. Elsevier, **2017**.

725   61.   Uto, K.; Tsui, J. H.; Deforest, C. A.; Kima, D. Dynamically tunable cell culture platforms for tissue
726   engineering and mechanobiology. *Prog. Polym. Sci.,* **2017**, *65*, 53–82.

727   62.   Klouda, L. Thermoresponsive hydrogels in biomedical applications A seven-year update. *Eur. J. Pharm.*
728   *Biopharm.* **2015**, *97*, 338–349.

729   63.   Olaru, A. M.; Marin, L.; Morariu, S.; Pricope, G.; Pinteala, M.; Tartau-Mititelu, L. Biocompatible chitosan
730   based hydrogels for potential application in local tumour therapy. *Carbohydr. Polym.* **2018**, *179*.

731   64.   Dou, Q.; Karim, A. A.; Loh, X. J. Modification of thermal and mechanical properties of PEG-PPG-PEG
732   copolymer (F127) with MA-POSS. *Polymers.* **2016**, *8*, 1–14.

733   65.   Al Khateb, K.; Ozhmukhametova, E. K.; Mussin, M. N.; Seilkhanov, S. K.; Rakhypbekov, T. K.; Lau, W.
734   M.; Khutoryanskiy, V. V. *In situ* gelling systems based on Pluronic F127/Pluronic F68 formulations for
735   ocular drug delivery. *Int. J. Pharm.* **2016**, *502*, 70–79.

736   66.   Akkari, A. C. S.; Campos, E. V. R.; Keppler, A. F.; Fraceto, L. F.; de Paula, E.; Tófoli, G. R.; de Araujo, D. R.
737   Budesonide-hydroxypropyl-cyclodextrin inclusion complex inbinary poloxamer 407/403 system for
738   ulcerative colitis treatment: Aphysico-chemical study from micelles to hydrogels. *Colloids Surfaces B*
739   *Biointerfaces* **2016**, *138*, 138–147

740   67.   Marcilli, R. H. M.; de Oliveira, M. G. Nitric oxide-releasing poly(vinyl alcohol) film for increasing dermal
741   vasodilation. *Colloids Surf. B* **2014**, *116*, 643–651.

742   68.   Taladriz-Blanco, P.; Pastoriza-Santos, V.; Pérez-Juste, J.; Hervés, P. Controllable nitric oxide release in the
743   presence of gold nanoparticles. *Langmuir* **2013**, *29*, 8061–8069.

744   69.   Zhou, X.; Wang, H.; Zhang, J.; Li, X.; Wu, Y.; Wei, Y.; Ji, S.; Kong, D.; Zhao, Q. Functional
745   poly(ε-caprolactone)/chitosan dressings with nitric oxide-releasing property improve wound healing.
746   *Acta Biomater.* **2017**, *54*, 128–137.

747   70.   Romić, M. D.; Klarić, M. Š.; Lovrić, J.; Pepić, I.; Cetina-Čižmek, B.; Filipović-Grčić, J.; Hafner, A.
748   Melatonin-loaded chitosan/Pluronic® F127 microspheres as *in situ* forming hydrogel: An innovative
749   antimicrobial wound dressing. *Eur. J. Pharm. Biopharm.* **2016**, *107*, 67–79.

750   71.   Wu, W.; Gaucher, C.; Fries, I.; Hu, X.; Maincent, P.; Sapin-Mineta, A. Polymer nanocomposite particles of
751   S-nitrosoglutathione: A suitable formulation for protection and sustained oral delivery. *Int. J. Pharm.* **2015**,

752   *495*, 354–361.

753   72.   Adams R. L. P. Cell culture for biochemists. 2 ed. New York: Elsevier, **1990**. 364p.

754   73.   Ammerman, N. C.; Beier-Sexton, M.; Azad, A. F. Growth and maintenance of Vero cell lines. *Curr. Protoc.*

755   *Microbiol.* **2008**.

756   74.   Fernández-Freire, P.; Labrador, V.; Pérez Martín, J. M.; Hazen, M. J. Cytotoxic effects in mammalian Vero

757   cells exposed to pentachlorophenol. *Toxicology*. **2005**, *210*, 1, 37-44.

758   75.   Ferraz, L. S.; Watashi, C. M.; Colturato-Kido, C. Pelegrino, M. T.; Paredes-Gamero, E. J.; Weller, R. B.;

759   Seabra, A. B.; Rodrigues, T. Antitumor potential of S-nitrosothiol-containing polymeric nanoparticles

760   against melanoma. *Mol. Pharmaceutics* **2018**, 10.1021/acs.molpharmaceut.7b01001

761   76.   Sanina, N.; Shmatko, N.; Stupina, T.; Balakina, A.; Terent'ev, A. NO-donor iron nitrosyl complex

762   with n-ethylthiourea ligand exhibits selective toxicity to glioma A172 cells. *Molecules*. **2017**, *22*, 1426. doi:

763   10.3390/molecules22091426.

764   77.   Lau, H. K.F. Cytotoxicity of nitric oxide donors in smooth muscle cells is dependent on phenotype, and

765   mainly due to apoptosis. *Atherosclerosis*. **2003**, *166* , 223 – 232.

766   78.   Huerta, S.; Chilka, S.; Bonavida, B. Nitric oxide donors: novel cancer therapeutics (review). *Int. J. Oncol.*

767   **2008**, *33*, 5, 909–927.

768   79.   Olguín, Y. et al., Effects of Liposomes Contained in Thermosensitive Hydrogels as Biomaterials Useful in

769   Neural Tissue Engineering. *Materials,* **2017**,*10,* 1122p.

770   80.   Park, K. M.;, Lee, S. Y.; Joung, Y. K.; Na, J. S.; Lee, M. C.; Park, K. D. Thermosensitive chitosan–

771   Pluronic hydrogel as an injectable cell delivery carrier for cartilage regeneration. *Acta Biomaterialia*, **2009**,

772   *5*, 1956–1965.

773   81.   Cellesi, F. Thermoresponsive hydrogels for cellular delivery. *Ther Deliv*. **2012**, *12*, 1395-1407.

774   82.   Choi, J. S.; Yoo, H. S. Pluronic/chitosan hydrogels containing epidermal growth factor with

775   wound-adhesive and photo-crosslinkable properties. *J. Biomed. Mater. Res. A.* **2010**, *95*, 564-73.

776   83.   Fu, Y.; Du, L.; Wang, Q.; Liao, W.; Jin, Y.; Dong, A.; Chen, C.; Li, Z. *In vitro* sustained release of

777   recombinant human bone morphogenetic protein-2 microspheres embedded in

778   thermosensitive hydrogels. *Pharmazie*. **2012**, *67*, 299-303.

779   84.   Radivojša, M. M.; Grabnar, I.; Gosenca, M.; Grabnar, P. A. Prolonged subcutaneous delivery of low

780   molecular weight heparin based on thermoresponsive hydrogels with chitosan nanocomplexes: Design,

781   in vitro evaluation, and cytotoxicity studies. *Int J Pharm*. **2015**, *488*, 127-135.

782   85.   Zhu, X.; Zhang, Y.; Huang, H.; Zhang, H.; Hou, L.; Zhang, Z. Functionalized graphene oxide-based

783   thermosensitive hydrogel for near-infrared chemo-photothermal therapy on tumor. *J. Biomater. Appl.*

784   **2016**, *30*, 1230-1241.

785   86.   Yasasvini, S.; Anusa R. S.; VedhaHari, B. N.; Prabhu, P. C.; RamyaDevi, D. Topical hydrogel matrix

786   loaded with Simvastatin microparticles for enhanced wound healing activity. *Mater. Sci. Eng. C. Mater.*

787   *Biol. Appl.*, **2017**, *72*, 160-167.

788   87.   Caramella, C. M.; Rossi, S.; Ferrari F.; Bonferoni, M. C.; Sandri, G. Mucoadhesive and thermogelling

789   systems for vaginal drug delivery. *Advanced Drug Delivery Reviews*, **2015**, *92*, 39–52.

790   88.   Machul, A.; Mikołajczyk, D.; Regiel-Futyra, A.; Heczko, P. B.; Strus, M.; Arruebo, M.; Stochel, G.; Kyzioł,

791   A. Study on inhibitory activity of chitosan-based materials against biofilm producing *Pseudomonas*

792   *aeruginosa* strains. *J. Biomater. Appl*, **2015**, *30*, 269–278.

793   89.   Lu, Y.; Slomberg, D. L.; Schoenfisch, M. H. Nitric oxide-releasing chitosan oligosaccharides as

794   antibacterial agents. *Biomaterials*, **2014**, *35*, 1716-1724.

795   90.   Kaye, K. S.; Pogue, J. M. Infections caused by resistant gram-negative bacteria: Epidemiology and
796   management. *Pharmacotherapy*, **2015**; *35*, 949–962.

797   91.   Dortet, L.; Boulanger, A.; Poirel, L.; Nordmana, P. Bloodstream infections caused by pseudomonas spp.:
798   How to detect carbapenemase producers directly from blood cultures. *J. Clin. Microbio.* **2014**, *52*, 1269–
799   1273.

800   92.   Kolpen, M.; Kuhl, M.; Bjarnsholt, T.; Hansen, C. R.; Liengaars, L.; Kharazmi, A.; Pressler, T.; Hoiby, N.;
801   Jensen, P. O. Nitrous oxide production in sputum from Cystic Fibrosis patients with chronic
802   pseudomonas aeruginosa lung infection. *Plos One*, **2014**, *9*, e84353.

803   93.   Loveday, H. P.; Wilson, J. A.; Kerr, K.; Pitchers, J. T.; Walker, J. Association between healthcare water
804   systems and *Pseudomonas aeruginosa* infections: a rapid systematic review. *J. Hosp. Infec.*, **2014**, *86*, 7-15.

805   94.   Mesaros, N.; Nordmann, P.; Plesiat, P.; Roussel-Delvallez, M.; Van Eldere, J.; Glupczynski, Y.; Van
806   Laethem, Y.; Jacobs, F.; Lebecque, P.; Malfroot, A.; Tulkens, P. M.; Van Bambeke, F. Pseudomonas
807   aeruginosa: resistance and therapeutic options at the turnof the new millennium. *Clin. Microbiol. Infect.*,
808   **2007**, *13*, 560–578.

809   95.   Hetrick, E. M.; Shin J. H.; Stasko, N. A.; Johnson, C. B.; Wespe, D. A.; Holmuhamedov, E.; Schoenfisch, M.
810   H. Bactericidal Efficacy of Nitric Oxide-Releasing Silica Nanoparticles. *ACS Nano*, **2008**, *2*, 235–246.

811   96.   Barraud, N.; Schlekeck, D.; Klebensberger, J.; Webb, J. S.; Hasset, D. J.; Rice, S. A.; Kjelleberg, S. Nitric
812   oxide signalling in pseudomonas aeruginosa biofilms mediates phosphodiesterase activity, decreased
813   cyclic di-GMP levels and enhanced dispersal. *J. Bacteriol.*, **2009**, *23*, 7333–7342.